Can slow electron holes exist?

I H Hutchinson

April 16, 2021

Abstract

One dimensional analysis is carried out of solitary positive potential structures whose velocity lies within the range of ion distribution velocities that are strongly populated: so called "slow" electron holes. It is shown that to avoid the self-acceleration of the hole velocity away from ion velocities it must lie within a local minimum in the ion velocity distribution. Quantitative criteria for the existence of stable equilibria are obtained. The background ion distributions required are generally stable to ion-ion modes unless the electron temperature is much higher than the ion temperature. Since slow positive potential solitons are shown not to be possible without a significant contribution from trapped electrons, it seems highly likely that such observed slow potential structures are indeed electron holes.

1 Introduction

Solitary positive potential structures are observed by satellites in some space plasmas to have speeds comparable to the typical ion thermal speed, even lying within the strongly populated velocities of the ion distribution[1–3]; that is what is meant here by calling the structures "slow". A candidate explanation of these structures is that they are "slow electron holes", in which the positive potential is sustained by a deficit of trapped electrons. However, till now it has been unclear theoretically whether, or under what circumstances, slow electron holes can exist. The purpose of the present study is to discover the theoretical conditions for the existence of plasma-sustained steady slow solitary positive potential structures, including electron holes, and identify the mechanisms that control them.

The reasons to question whether slow electron holes can exist are to do with the interaction of their positive potential peak with the ions. Classic electron holes move at speeds, relative to ions, up to of order the electron thermal speed v_{te}[4, 5]. And when they are at more than a very small fraction of v_{te}, the ion perturbation is small because the duration of any moving electron hole's interaction with an ion is much smaller than the typical response time of the (far heavier) ions. Ion response can then often be completely ignored. For slower holes, though, ion interaction gradually becomes important. When hole speed is less than a few (up to about $(m_i/m_e)^{1/4}$) times the ion acoustic speed ($c_s = \sqrt{T_e/m_i}$), the ion interaction is significant, and the the electron hole speed is "repelled" from the ion speed[6, 7], maintaining a velocity (difference) greater than a minimum that increases with hole potential. If the hole speed is less than that minimum, an oscillatory instability in the hole speed arises[8]

and there is therefore a forbidden region of hole speed. This forbidden velocity region has a lower limit that is at approximately the ion-acoustic soliton speed, which is of order c_s (depending on peak potential[1]). At that specific speed, an entity usually called a coupled hole-soliton (CHS) is known from simulations[9–11] to exist. In effect the electron hole is trapped in, and enhances, the positive potential produced at that speed by the positive ion density perturbation of the ion acoustic soliton. A CHS generally moves faster than the ion thermal speed, provided the electron temperature is greater than ion temperature, so there are few ions in the distribution at the CHS speed, and Landau damping can be small.

It is emphasized that none these known types of theoretical holes qualifies for the present meaning of "slow". Neither do holes produced by the Bunemann instability when there is substantial drift between ion and electron populations, invoked by Norgren et al[12, 13] to explain their space observations. Holes produced[11, 14, 15] by Bunemann instability usually have speeds (relative to ions) $\ll v_{te}$ but not $< c_s \simeq \sqrt{m_e/m_i}\, v_{te}$, let alone $\sim v_{ti}$. Instead, the present paper addresses the "Group 3" electron holes observed by Steinvall et al[2] ("on the magnetospheric side of the magnetopause") that have speeds relative to ions below c_s (Group 1 speeds exceed the oscillatory instability threshold, and Group 2 are consistent with being CHS type). A fraction of the observations of Graham et al[1] ("near the magnetopause") and of the blue points in Figure 4 of Lotekar et al[3] (magnetotail) also are slow in the present sense.

Simulations that initialize an electron hole at speeds of order the ion thermal speed v_{ti} or less, observe a remarkable and rapid "self-acceleration" of the hole[7, 9, 16–18]. The growing negative ion density (and hence charge) perturbation caused by the repulsion of ions from the positive potential of the hole repells the electron hole, because an electron hole's dynamics as a composite entity are such that it has an effective charge to mass ratio equal to that of the electron[6, 19]. A short time after initialization, it moves away at speeds much larger than v_{ti}. Thus, past simulation attempts have failed to produce steady slow electron holes.

The novelty and complexity of the present analysis in comparison with the prior treatments of ion acoustic solitons and electron holes is that it *requires a kinetic* (rather than fluid, e.g.[20]) treatment of the ions in equilibrium. Concerning past kinetic electron hole analysis (e.g.[21]) and simulations (e.g.[17]), the key difference is that the present analysis shows that for *slow* positive structures to exist stably the background ion velocity distribution generally cannot be "single-humped". It must instead possesses at least two maxima. Indeed, it is shown that slow positive solitary potentials sustained by trapped electron deficit (1) cannot persist in single-humped ion distributions; (2) can persist only when the velocity of the electron hole lies in a local minimum of the ion distribution function; but (3) do not require background distributions that are ion-ion unstable, provided the electron temperature is not very high. All the discussion here is one-dimensional, and multidimensional stability is beyond the present scope. The conclusion therefore is that, from a one-dimensional perspective, slow electron holes can exist, requiring distinctively non-thermal external ion distributions; but those distributions are not themselves unstable and can therefore persist for substantial time durations.

These theoretical characteristics are valuable for identifying the nature of slow solitary

[1]Conventionally the cold ion acoustic soliton maximum speed is taken as $1.59c_s$ at potential $\phi = 1.26T_e/e$, but that is for an isothermal (Boltzmann) electron response, whose nonlinear application is debatable.

potential peaks observed in plasmas, and for indicating the presence of double-humped ion distributions. Recent analysis of observations reported elsewhere [Kamaletdinov et al 2021, in preparation] confirm the characteristics for slow electron holes observed in the plasma sheet boundary layer.

Section 2 addresses ion distribution functions that have reflectional symmetry in some reference frame. The simplifications of symmetry make it easier to understand the concepts introduced and permit straightforward proofs concerning stability and equilibrium. Section 3 generalizes these results to asymmetric ion distributions, and section 4 addresses the question of the linear stability of the uniform background ion distributions found to be necessary for the existence of slow electron holes.

2 Symmetric Distribution Functions

Consider a steady solitary positive potential structure in one dimension: $\phi(x)$, possessing a single maximum $\phi = \psi$ at position $x = 0$, and tending to the same potential $\phi = \phi_\infty = 0$ at distant positions $x \to \pm\infty$. For motion in this single dimension, suppose the distribution function of ions approaching the potential structure from the distant plasma to be given as $f_\infty(v_\infty)$, in a frame of reference in which the structure is stationary.

A collisionless ion equilibrium satisfies the steady Vlasov equation, giving conservation of distribution function and energy on orbits, leading to

$$f(x,v) = f_\infty(\infty, v_\infty) \qquad \text{where} \qquad v^2/2 + \phi(x) = v_\infty^2/2 + \phi_\infty. \tag{1}$$

In this paper, to abbreviate the equations we mostly work in conveniently scaled units: energy normalized to thermal energy for a reference temperature T_0, length normalized to Debye length $\lambda_D = \sqrt{\epsilon_0 T_0/e^2 n}$, and velocity to ion thermal speed $\sqrt{T_0/m_i}$. In these units, the ion mass and charge are unity. Where numerical values of quantities like distribution function, density, or force-density etc., are presented, they are for unit background density n_∞.

When the ion distribution function *in the rest frame of the structure* is not symmetric, very substantial analytic complications nevertheless arise from ion reflections. We shall address these in a subsequent section, but initially it is simpler to exclude those complications by assuming the distribution to be reflectionally symmetric in ion velocity v.

2.1 Single-Humped Distributions: Density in Equilibrium

Since $f_\infty(v_\infty)$ is symmetric in the sign of v_∞, using $vdv = v_\infty dv_\infty$ one can simply write the (ion) density as

$$n = 2\int_{|v_\phi|}^{\infty} f_\infty \frac{v_\infty dv_\infty}{\sqrt{v_\infty^2 - v_\phi^2}} = 2\int_{|v_\phi|}^{\infty} f'_\infty \sqrt{v_\infty^2 - v_\phi^2}\, dv_\infty, \tag{2}$$

where $|v_\phi| = \sqrt{2(\phi - \phi_\infty)}$ is the speed at infinity of ions that are reflected at the position x, potential ϕ, and prime denotes differentiation with respect to argument (v_∞). This density

is then simply a function of ϕ. Express the density far from the potential structure as

$$n_\infty = 2\int_0^\infty f_\infty dv_\infty = -2\int_0^\infty f'_\infty v_\infty dv_\infty, \tag{3}$$

and so deduce the density change introduced by the presence of the potential structure:

$$n - n_\infty = 2\int_0^{|v_\phi|} f'_\infty v_\infty dv_\infty + 2\int_{|v_\phi|}^\infty f'_\infty \left[v_\infty - \sqrt{v_\infty^2 - v_\phi^2}\right] dv_\infty. \tag{4}$$

When f_∞ has only a single maximum (at $v = 0$) f'_∞ is negative throughout the integrals. The functions multiplying f'_∞ in the integrands are everywhere positive; so for symmetric single-humped f_∞, we have $n < n_\infty$: the ion density change arising from a positive potential is always negative. This is one indication that a positive potential soliton sustained by ions cannot exist at low speed relative to the ion thermal (or acoustic) speed. The density perturbation has the wrong polarity for self sustainment. What is more, this observation has important consequences for the possibility of slow electron holes. For single-humped f_∞ they will have negative ion charge relative to the external plasma. This negative ion charge repells the electron hole that causes them. The result is rapid acceleration of the electron hole until it has speed higher than typical ion thermal speeds. Such unstable acceleration has been well documented in simulations[7, 17][2]. Thus the slow electron hole equilibrium in a single-humped ion distribution is unstable to hole acceleration.

2.2 Force and acceleration of the potential structure

To make a more quantitative assessment of slow hole dynamics, it is simplest to find the total force exerted on the ions by the entire potential profile $\phi(x)$ (per unit area perpendicular to x). Evidently it is $F = \int \rho E dx = -\int_{-\infty}^{\infty} n(x)\frac{d\phi}{dx}dx = -\int n(\phi)d\phi$. When f_∞ is symmetric, $n(\phi)$ is independent of the sign of x, denoted σ_x, while $d\phi/dx$ has sign $-\sigma_x$. Therefore, in steady state regardless of the shape of $\phi(x)$, the total force on the ions is zero, as a consequence of symmetry. Perhaps more significantly, the reaction force exerted by the ions on the potential structure ($-F$) is also zero. It is in equilibrium.

Suppose, however, that the potential structure is stationary $\phi_0(x)$ (in the equilibrium frame) and remains in steady equilibrium long enough for the ion density to reach the value given by eq. (2); but then some perturbative uniform displacement δx of the potential structure (in the equilibrium frame) begins, which is rapid relative to the timescale of adjustment of the ion density to the movement. This presumption is a good approximation for an electron hole experiencing unstable acceleration because the timescale for electron motion and hence structure motion is so much shorter (by $\sim \sqrt{m_e/m_i}$) than for ion motion. After a short time, the density of the slowly responding ions, $n(x)$, will to lowest order be unchanged, it remains a function of the steady potential ϕ_0, but will no longer be a function of the instantaneous potential $\phi = \phi_0 + \delta\phi$. Consequently the symmetry is broken, and total force

[2] A recent paper[22] reports Vlasov simulations appearing to show for Maxwellian distributions at $T_i/T_e = 10$ that self-acceleration is suppressed, and claims that high enough ion temperature $T_i/T_e > 3.5$ can reverse the ion density response. These claims are proven by the present simple derivation to be incorrect. The simulation code used is not self consistent and its results are contradicted by simulations using a well established code. The analysis included to explain its results is faulty.

on the ions will be non-zero. The linearized perturbation for a small rigid shift δx of the potential structure is $\delta\phi \simeq -\frac{d\phi_0}{dx}\delta x$ which is anti-symmetric. The ion force increment is

$$\delta F = -\int n(x)\frac{d\delta\phi}{dx}dx = \delta x\int n(x)\frac{d^2\phi_0}{dx^2}dx = -\delta x\int \frac{dn}{dx}\frac{d\phi_0}{dx}dx = -\delta x\int \frac{dn}{d\phi_0}\left(\frac{d\phi_0}{dx}\right)^2 dx. \tag{5}$$

Now the potential structure has been displaced from equilibrium and experiences a force $-\delta F = -C\delta x$, where the coefficient is $C = \delta F/\delta x = -\int \frac{dn}{d\phi_0}\left(\frac{d\phi_0}{dx}\right)^2 dx$. Incidentally, this force is related to imbalanced reflection of the ions from the potential structure and ion jetting. Imbalanced reflection of electrons from small negative-potential *ion holes* is proportional to the slope of the electron distribution function at the hole speed[23]. But for positive structures it is better to express the force in terms of these instantaneous integrals, since full reflection of ions takes much longer to transfer their momentum to the structure than the timescale of hole motion. Whether or not the structure regarded as a rigid composite object continues to be displaced or returns to its equilibrium position depends upon the sign of its acceleration, and hence on the sign of C, which is evidently minus the sign of $dn/d\phi_0$ (averaged over the hole with positive definite weight); but it also depends on the structure's response to force, that is, its effective mass M.

Supposing the potential structure to be an electron hole, one can deduce the acceleration of the hole by requiring the total of electron ($\dot{P}_e$) and ion ($\dot{P}_i$) momentum rates of change to be zero (since the electric field momentum is negligible): $0 = \dot{P}_i + \dot{P}_e = \delta F + \dot{P}_e$. Thus the effective mass of the hole, its force divided by acceleration, is $M = -\delta F/\ddot{\delta x} = \dot{P}_e/\ddot{\delta x}$. The electron momentum change arises from jetting by the accelerating potential structure, and is given by equation (34) of reference [6] in dimensional units

$$\dot{P}_e = -\ddot{\delta x}\, n_e m_e \int h(\chi)dx, \tag{6}$$

where $h(\chi)$ is a non-negative function[3] of argument $\chi \equiv \sqrt{|e\phi|/T_e}$. For negligibly shifted Maxwellian electrons h can be written in closed form as

$$h(\chi) = -\frac{2}{\pi}\chi + \left[\left(2\chi^2 - 1\right)\mathrm{e}^{\chi^2}\mathrm{erfc}(\chi) + 1\right]. \tag{7}$$

The effective electron hole mass (per unit transverse area) $M = -n_e m_e \int h(\chi)dx$ is thus negative.

Within the present lumped approximation the equation of motion of the potential structure is $\ddot{\delta x} = -(C/M)\delta x$, giving eigenfrequency $\omega = \pm\sqrt{C/M}$. The *stability* of the initial symmetric equilibrium depends on the sign of C/M. Stable oscillation is expected for C/M positive, exponential growth for C/M negative. When ion density is decreased by positive potential, $dn/d\phi_0 < 0$, C is positive. Therefore C/M is negative and the hole is unstable to displacements relative to the equilibrium position and velocity when ion density change

[3]Strictly, eq. (7) applies when ion charge response is neglected. That neglect is not immediately obvious for slow holes. However, at the threshold of instability the ion charge response actually *is* negligible, so it is appropriate to invoke the equation for thresholds, as well as for order of magnitude γ-estimates for small amplitude holes.

caused by positive potential is negative, as it is for symmetric single-humped ion distribution function.

The mass of a hole of small ψ can be calculated using the approximation $h(\chi) \to \chi^2 = \phi T_0/T_e$ so in dimensional units $M = -(n_e m_e/T_e)\int e\phi dx$, and

$$\frac{C}{M} = \frac{-e\int \frac{dn}{d\phi_0}\left(\frac{d\phi_0}{dx}\right)^2 dx}{-(n_e m_e e/T_e)\int \phi dx}. = \frac{-e\int \frac{dn}{d\phi_0}\left(\frac{d\phi_0}{dx}\right)^2 dx}{-(n_e m_e e/T_e)\int \phi dx}. \tag{8}$$

Now we convert ϕ, ψ, x, and C/M into dimensionless units dividing them by T_0/e, λ_D, and ω_{pi}^2 respectively, and defining an effective dimensionless hole length $L \equiv \int \phi dx/\psi$. This yields the dimensionless form

$$\frac{C}{M} = \frac{-e\int \frac{dn}{d\phi_0}\left(\frac{d\phi_0}{dx}\right)^2 dx}{-(n_e m_e e/T_e)\int \phi dx} \times \frac{1}{\lambda_D^2 \omega_{pi}^2} \simeq -2\frac{T_e}{T_0}\frac{m_i}{m_e}\frac{\psi}{L^2}, \tag{9}$$

where, anticipating a result to be shown in the next section, the dimensionless magnitude of the numerator for hole form $\psi\,\mathrm{sech}^4(x/\ell)$ and unit density Maxwellian ions is found to be approximately $C = 2\psi^2/L$. A self-consistent electron hole of the sech^4 form has length $L = (16/3)\lambda_{De} = (16/3)\sqrt{T_e/T_0}$ (dimensionless). Therefore $C/M = -(3/16)^2 2\psi(m_i/m_e)$ and the growth rate is $\gamma = \sqrt{2\psi m_i/m_e}(3/16)$ in ω_{pi} units. It is perhaps more intuitive to write dimensionally

$$\gamma \simeq \frac{3}{16}\sqrt{\frac{2e\psi}{T_0}}\,\omega_{pe}. \tag{10}$$

This confirms that the instability is fast because it is on the electron time-scale ω_{pe}^{-1} rather than the ion timescale, hence justifying the model taking stationary ions during the motion of the potential structure. But if ψ is very small, the gap between the reduced γ and the ion response time will eventually disappear, and the approximation become inadequate.

2.3 Non-single-humped Distribution Function Hole Stability

For a stable electron hole or other positive potential structure attributable to the plasma itself to exist, we require the ion density perturbation that it produces to be non-negative. This is achieved in classic ion acoustic solitons by the relative speed of the soliton and the ions being substantially larger than the ion thermal speed. A classic soliton is not slow in the current sense; and also the ion velocity distribution is not symmetric (in the structure frame) but consists of a single Maxwellian shifted by velocity v_b. Pursuing in this section only symmetric distributions, one can clearly make the distribution symmetric by introducing a symmetric second ion population of shift $-v_b$. In that case a soliton can exist, but physically it is still not "slow" in the sense of the structure velocity coinciding with the dominant part of the ion distribution.

This two-beam soliton situation shows qualitatively how to obtain positive ion density perturbation. Ions that are not reflected, because their energy exceeds the peak potential, contribute positively to the ion density perturbation because their speed $|v|$ at positive potential is lower than at ϕ_∞ (conserving energy) yet their flux (nv) must be independent of position; so n must increase to compensate. A passing monoenergetic beam of ions has

density $n(\phi) = n_\infty v_\infty / \sqrt{v_\infty^2 + 2(\phi - \phi_\infty)}$, which increases without bound near the potential $\phi = \phi_\infty + v_\infty^2/2$ needed for reflection. Therefore, if the unreflected (passing) ion population is sufficiently dominant, the ion density change is positive. What the previous subsection showed is that for *single-humped* symmetric distributions the passing population is never sufficiently dominant. A sufficiently widely spaced two-beam distribution can, however, achieve sufficient dominance. If the spacing $2|v_b|$ is reduced, eventually that dominance will be lost and the unstable negative ion density change $[n - n_\infty]$ will reappear. The intuitive question therefore is quantitatively how small can the beam spacing be and still avoid instability. We already know from the previous subsection that part of the answer is that the distribution must be non-single-humped; in other words that it must have a local minimum. But how deep must the minimum be?

The stability threshold is determined, on the basis of the lumped treatment of electron-sustained structure motion, by the change of sign of the force coefficient, $C = \delta F/\delta x = -\int \frac{dn}{dx}\frac{d\phi_0}{dx}dx = -\int \frac{dn}{d\phi_0}\left(\frac{d\phi_0}{dx}\right)^2 dx$. Instability arises if $\delta F/\delta x$ is positive. Its value is determined by both the distribution function, giving $n(\phi_0)$, and potential profile $\phi_0(x)$, giving $\frac{d\phi_0}{dx}$. However its sign depends only on the relative shape of $\phi_0(x)$, not on its extent, because expanding or contracting the profile in x by a uniform (positive) scale factor ℓ simply divides $\delta F/\delta x$ by ℓ. Thus, for example, a Gaussian potential $\phi = \psi e^{-x^2/\ell^2}$ will give a very slightly different threshold than $\phi(x) = \psi\,\mathrm{sech}^4(x/\ell)$, but neither threshold depends on the value of ℓ. We choose ℓ conveniently so as to make $L \equiv \int \phi dx/\psi = 1$, requiring $\ell = 3/4$ for the $\mathrm{sech}^4(x/\ell)$ shape, in the following plots. Using instead a Gaussian with $\ell = 1/\sqrt{\pi}$ gives plots that appear so similar they are not worth including. To an excellent approximation only the overall width L and height ψ of the hole control the quantitative values.

To evaluate $\delta F/\delta x$ (numerically) for a specified distribution and potential shape, we must obtain $n(\phi)$ by integrating eq. (2) with respect to v_∞ and then integrate $\int \frac{dn}{dx}\frac{d\phi_0}{dx}dx$ with respect to x, for the chosen shape $\phi(x)$. A code has been written to perform these integrations for arbitrary (input) f_∞ or for distributions consisting of multiple shifted Maxwellian components where their separation (and hence the depth of the local minimum) is scanned.

For distributions consisting of two symmetric Maxwellian components, shifted from $v = 0$ by $\pm v_b$, Fig. 1(a) shows ion distribution shapes as v_b is varied, with the marginally stable cases for $\psi = 0.02$ and $\psi = 0.5$ emphasized in bold black and red. Fig. 1(b) shows the force coefficients $\delta F/\delta x/\psi^2$ (using $L = 1$) as a function of beam shift v_b for a range of potential heights ψ. The magnitude of $\delta F/\delta x$ scales approximately like ψ^2 but because of nonlinearities in $n(\phi)$ there is a small variation in the force and threshold with potential peak height.

As shown in Fig. 1(b), over a wide range of potential heights ψ the threshold v_b, where $\delta F/\delta x$ crosses zero, varies a modest amount: between 1.33 and 1.5, and the corresponding depth of the minimum $(f_{max} - f_{min})/f_{max}$ is a fraction of the f-maximum that lies between 0.20 and 0.36. Greater ψ requires deeper minimum.

Fig. 2(a) shows for reference the used sech^4 potential profile including the small shift δx used for calculating δF. Fig. 2(b) shows the (unshifted) corresponding first stable density profile (blue) and the adjacent last unstable density profile (green) in which the v_b is smaller by 0.02. The precise threshold lies between these two $n(x)$ profiles, corresponding to a density that is nearly flat (but not exactly because of profile and nonlinear effects). Fig. 2(c)

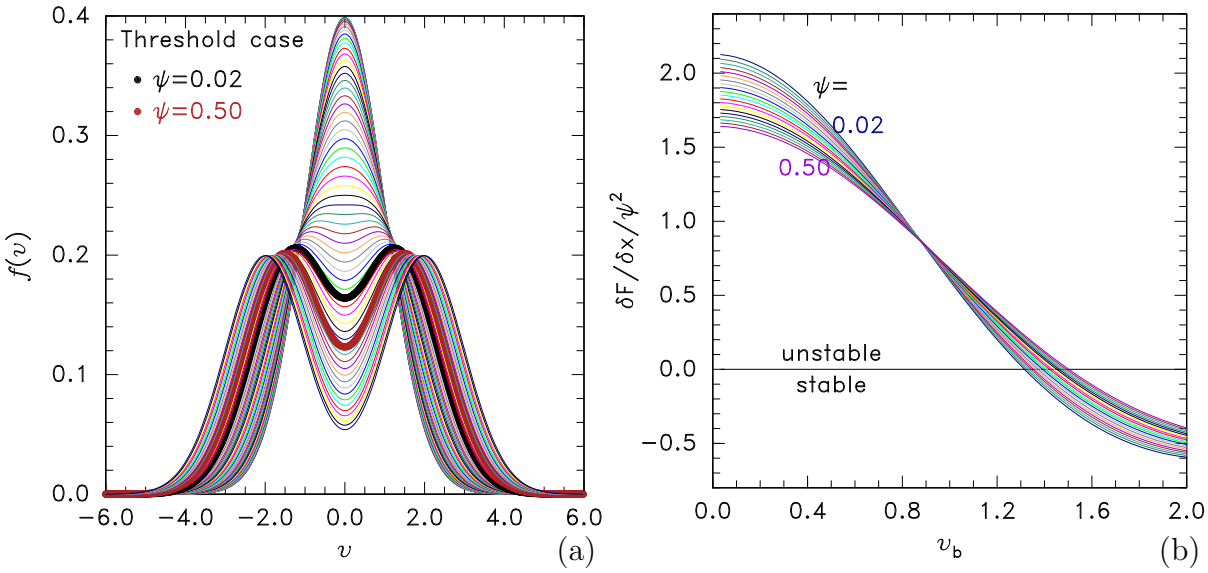

Figure 1: (a) The ion distribution functions arising for the sum of two symmetric Maxwellians displaced by $\pm v_b$ for $0 < v_b < 2$. The threshold case is marked in black for $\psi = 0.5$ and red for $\psi = 0.02$. (b) The force coefficient $\delta F/\delta x/\psi^2$ as a function of the beam velocity for an equally spaced range of (Gaussian) electron hole potential heights ψ.

shows the same thing for a much larger potential peak ψ. One can see that near threshold $dn(\phi)/d\phi$ actually reverses its sign at large ϕ.

2.4 Positive potential structures sustained by ions?

Since within a local $f_\infty(v)$ minimum a positive potential gives positive ion charge, one might wonder whether such an effect can by itself be responsible for sustaining the structure. In multiple-humped ion distributions is there such a thing as a slow positive ion soliton? The answer appears to be no. The reason is not stability, but equilibrium. To generate a solitary positive potential peak requires the electric charge to be positive near the peak but negative in the wings. Yes, ion charge perturbation can be positive for positive potential in a local minimum of the distribution function, but it is never negative, and actually $dn/d\phi$ decreases with increasing ϕ. Therefore certainly ions alone cannot sustain a slow positive soliton. This contrasts with negative potential *ion holes*, which can be sustained by a deficit of trapped ions.

A Maxwellian electron distribution with no trapped deficit gives a negative charge density perturbation approximately linear with potential ($\sim -\phi$). Electrons can therefore give the required negative charge density in the wings of the hypothesized solitary structure, and do so for a classic ion-acoustic soliton. But to obtain positive charge density near the potential peak, the rise in ion density has to overwhelm the rise in electron density in the center but not in the wings. That requires the ion density to have substantial positive curvature $d^2n/d\phi^2$. It has for a passing ion beam, but it generally does not for a slow structure, because of ion reflection. In fact (compare Fig. 2(c)) at potentials comparable to the width of the $f(v)$ minimum, $n(\phi)$ has substantial *negative* curvature, with $dn/d\phi$ eventually becoming

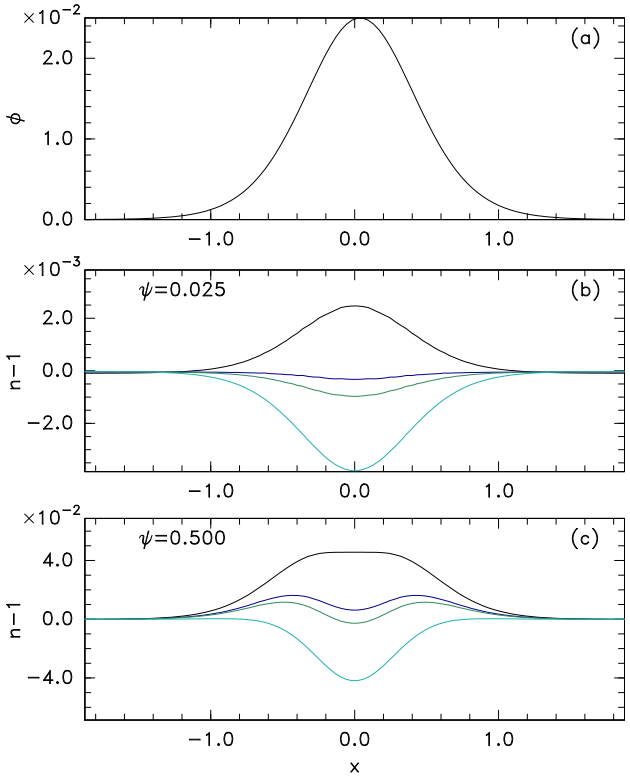

Figure 2: (a) Slightly shifted Gaussian potential profile to calculate δF. (b) Ion density as a function of position for the first stable (dark blue) and last unstable (green) velocity shift v_b, for peak potential $\psi = 0.5$, together with cases more stable (black greater v_b) and more unstable (light blue smaller v_b). (c) Ion density threshold cases like (b) but for greater ψ.

negative.

Therefore essentially any positive solitary structure that is slow in the sense of having velocity coinciding with the dominant parts of the ion distribution cannot be sustained by ions alone, and cannot be sustained at all unless the electron distribution changes make major contributions to the central positive charge. This restriction is not exactly a watertight proof that positive slow solitary structures are electron holes, but it closes off most plausible alternative possibilities.

3 Asymmetric Distribution Functions

Now we must tackle asymmetric ion velocity distributions and their complications.

3.1 Calculation of density

First, if f_∞ is asymmetric in the incoming sign (σ_∞ say) of v_∞, the ion density will be a function of *both* the magnitude of the potential *and* the side of potential peak at which the potential occurs. That is because slow ions will be reflected and hence contribute only on one side or the other of the peak (positions x having sign $\sigma_x = -\sigma_\infty$). We should therefore refer to the potential in a way that indicates the sign; one convenient way to do so is to express it as the distant incoming velocity that reflects at ϕ: $v_\phi \equiv -\sigma_x\sqrt{2(\phi-\phi_\infty)} = \sigma_\infty\sqrt{2(\phi-\phi_\infty)}$.

But second, even with this clarification, the density is actually a function of the local potential (and hence v_ϕ) *and also* the height of of the potential peak ψ; because although in a collisionless situation f and energy are constant, whether the distribution of particles $f(x,v)$ moving away from the peak is representative of v_∞ positive or negative depends whether those particles have been reflected or have passed over the peak.

So at potential ϕ whose position sign is given by $-v_\phi$, the exiting particles (v and x having the same sign) have $f_\infty(v_\infty)$ corresponding to a sign of v_∞ equal to $\mp\sigma_x$, depending on whether they have been reflected or not. That is, for $v^2/2+\phi > \psi$ (passing particles), $f(x,\sigma_x|v|) = f_\infty(-\sigma_x\infty, \sigma_x\sqrt{v^2+2[\phi-\phi_\infty]}\,)$, while for $v^2/2+\phi < \psi$ (reflected particles), $f(x,\sigma_x|v|) = f_\infty(\sigma_x\infty, -\sigma_x\sqrt{v^2+2[\phi-\phi_\infty]}\,)$. Since I find this distinction requires considerable care, I illustrate it graphically in Fig 3, denoting $v_\psi = \sqrt{2(\psi-\phi_\infty)}$ (positive value). The v_∞ ranges that contribute to the density locally at $\phi(x)=\phi$ for the two signs $\sigma_\infty = +1$ ($\sigma_x = -1$) blue, and $\sigma_\infty = -1$ ($\sigma_x = +1$) red are shown as horizontal dash-dot lines. A purely illustrative Maxwellian f_∞ is shown emphasizing that even a shift of a symmetric Maxwellian from the structure velocity (zero) gives rise to asymmetry, and hence dependence of density on ψ.

The density is given as before by

$$\int f(v)|dv| = \int f_\infty \frac{|v_\infty|}{|v|}|dv_\infty| = \int f_\infty \frac{|v_\infty|}{\sqrt{v_\infty^2 - v_\phi^2}}|dv_\infty|, \tag{11}$$

using $vdv = v_\infty dv_\infty$ and $v_\phi^2 \equiv 2(\phi-\phi_\infty)$, but the tricky part is the three subranges of integration. They give density contributions we may denote n_r from particles that will be or have been reflected giving two contributions from velocity in $[v_\phi, \sigma_\infty v_\psi] = [v_\phi, -\sigma_x v_\psi]$, n_t

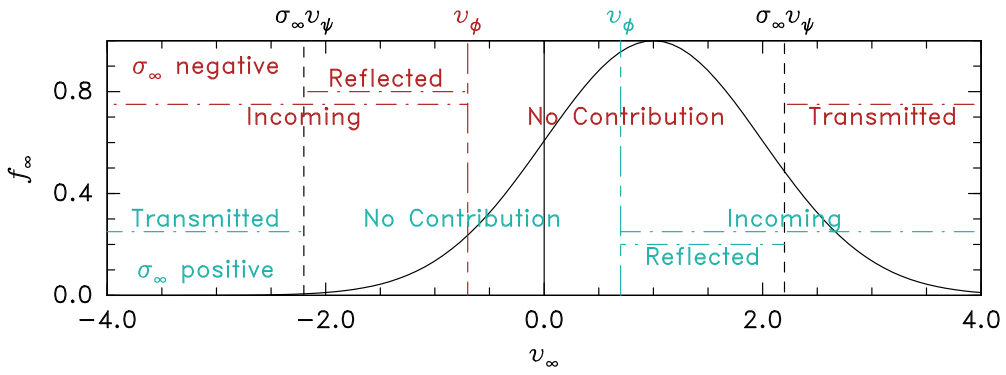

Figure 3: Distant velocity ranges (v_∞, horizontal dash-dot lines) that contribute to the integrals of $f_\infty(v_\infty)$ giving density, at the two sides of a potential peak: $\sigma_\infty = +1$ (x negative) blue, and $\sigma_\infty = -1$ (x positive) red. Vertical lines at v_ϕ indicate the v_∞ that reflects at potential ϕ and v_ψ that reflects at ψ

from particles that have been transmitted $[\sigma_x v_\psi, \sigma_x \infty]$, and n_u (unreflected) from particles that will not be reflected $[-\sigma_x v_\psi, -\sigma_x \infty]$:

$$n = n_r + n_t + n_u = \left[2\int_{v_\phi}^{-\sigma_x v_\psi} + \int_{\sigma_x v_\psi}^{\sigma_x \infty} + \int_{-\sigma_x v_\psi}^{-\sigma_x \infty} \right] f_\infty \frac{|v_\infty|}{\sqrt{v_\infty^2 - v_\phi^2}} |dv_\infty|. \tag{12}$$

Since each integration range is increasing in absolute value, the sign of dv_∞ is the same as the sign of v_∞; so $|v_\infty||dv_\infty| = v_\infty dv_\infty$ and we need not take moduli. For numerical evaluation it is advantageous as before (eq. 2) to integrate by parts to remove the singularity at $v_\infty^2 = v_\phi^2$, giving

$$\begin{aligned} n =& [f_\infty(-\sigma_x v_\psi) - f_\infty(\sigma_x v_\psi)]\sqrt{v_\psi^2 - v_\phi^2} \\ &- \left[2\int_{v_\phi}^{-\sigma_x v_\psi} + \int_{\sigma_x v_\psi}^{\sigma_x \infty} + \int_{-\sigma_x v_\psi}^{-\sigma_x \infty} \right] f'_\infty \sqrt{v_\infty^2 - v_\phi^2}\, dv_\infty, \end{aligned} \tag{13}$$

in which the integrated parts no longer cancel.

This expression allows us to calculate the density arising everywhere on a potential structure stationary in some inertial frame and the resulting force on the ions $F = -\int_{-\infty}^{\infty} n(x)\frac{d\phi}{dx}dx$. However, unlike the symmetric case, no symmetry now tells us what the equilibrium velocity of that frame relative to the ion distribution should be. And for an arbitrary frame velocity v_h relative to the ion distribution, there will generally be a nonzero ion force $F(v_h)$. Then the configuration will not be in equilibrium because the structure potential will be subject to a net force $-F$. Only for the particular structure velocity that makes $F(v_h) = 0$ will there be an equilibrium. (This is true also for a distribution like a sum of two similar but shifted Maxwellians, that has velocity symmetry in *some other* frame of reference; but we previously tacitly adopted that particular frame of reference as our equilibrium structure frame.)

3.2 Hole positional stability

For f_∞ intrinsically asymmetric we need to find both the equilibrium electron hole velocity (potential structure velocity), v_{h0}, and the derivative of the force with respect to a shift of the structure relative to its equilibrium position, $\delta F/\delta x$, to determine the equilibrium's stability to rapid motion of the potential structure leaving behind a fixed ion density. However before we do that, a second factor concerning stability arises in respect of dF/dv_h. If we find an equilibrium hole velocity, which has $F = 0$, then how does F vary when we consider a neighboring hole *velocity* (not *position*)? This question governs the stability of the situation for slow hole acceleration in the opposite limit where the ion density perturbation accelerates with the potential structure. If F changes in such a direction as to oppose the acceleration, the equilibrium is stable to such acceleration; but if not then the equilibrium is unstable. Of course, in reality the two types of hole motion, having stationary ion density, or having perfectly tracking ion density, are approximate extreme limits of a continuous response dependent on frequency. Full frequency analysis proves to be mathematically challenging even for an ion stream that is well separated from the hole velocity, but has been completed showing oscillatory instability for hole speed down to a few ion sound speeds[8]. In the present work we content ourselves instead with the combination of a more heuristic pair of approximations: the extreme limits of fast and slow. This renders stability criteria but not precise eigenvalues.

We can formulate a lumped parameter treatment by supposing that we can combine the two different perturbations of the ion force arising from the coefficients $\delta F/\delta x$ and $dF/dv_h = dF/d\dot{x}$ into a second order system: $M\dot{v}_h = M\ddot{x} = (\delta F/\delta x)x + (dF/d\dot{x})\dot{x}$, which has the form:

$$\ddot{x} + \frac{dF}{Md\dot{x}}\dot{x} + \frac{\delta F}{M\delta x}x = \ddot{x} + b\dot{x} + cx = 0. \tag{14}$$

The solutions of this linear second-order equation are stable if and only if both c and b are non-negative. In that case, it is a damped harmonic oscillator equation. When instead c is negative, then an exponentially growing solution dominates the long-time behavior. If c is positive but b is negative, a growing oscillation is the instability. Stability of the electron hole requires both $c = C/M = \frac{\delta F}{M\delta x}$ and $b = \frac{dF}{Mdv_h}$ to be positive. And since M is negative that means the two ion force derivatives must be negative.

Finding a stable equilibrium is carried out as follows. For a given distribution, the structure velocity v_h is scanned in small steps relative to the ion distribution to find the first (and usually the only) value at which the force F changes from positive to negative ($dF/dv_h < 0$, making b positive) *and also* the value of $\delta F/\delta x$ is negative so c is positive (i.e. stable). If no such v_h is found, the distribution does not permit stable slow electron holes.

The other major approximation we make here is that we do not calculate self-consistently the form of the electron hole potential $\phi(x)$. For symmetric distributions, in principle we could choose it to be whatever we like and find the required self-consistent trapped electron distribution through the integral equation analysis of Bernstein, Greene, and Kruskal[5, 24]. Since here we are calculating the effects on a known potential of the interaction with the ions, it is sufficient just to prescribe the potential, especially since as noted in section 2.3 the detailed shape of the potential has only a rather weak effect. However, for asymmetric ion distributions and finite hole peak potential ψ, it is no longer the case that the ion density

is the same on the two sides of the electron hole. Therefore it is far from obvious that the potential need be the same on the two sides either. When it is not and ϕ_∞ is different for $\pm\sigma_x$, the potential structure has the form of a non-monotonic double layer[25] and many additional complexities arise, which it is not the purpose to address here. Therefore we continue by setting aside these complications, assuming a symmetric potential form $\phi(x) \propto \mathrm{sech}^4 x$ and limiting the applicability of the present result to electron holes or other structures that have negligible net potential drop across them, which will be formally justified if the peak potential is small.

The specific distribution shapes considered here are adequately represented by the sum of two Maxwellian components shifted from each other by $2v_b$. The widths and relative densities of the two components can be prescribed so as to represent different generic shapes. The shift parameter v_b determines how deep any local minimum in the distribution is. The threshold value of v_b, at which stable electron holes become permitted, is found by the following outer iteration of the above described structure velocity v_h scan. A relatively coarse v_b scan is carried out over a range sufficient to cover all desired distributions, and the smallest v_b that permits a stable equilibrium is found. An example scan is shown by the different colored lines in Fig. 4. The threshold v_b is then refined by setting the last v_b that did not permit an

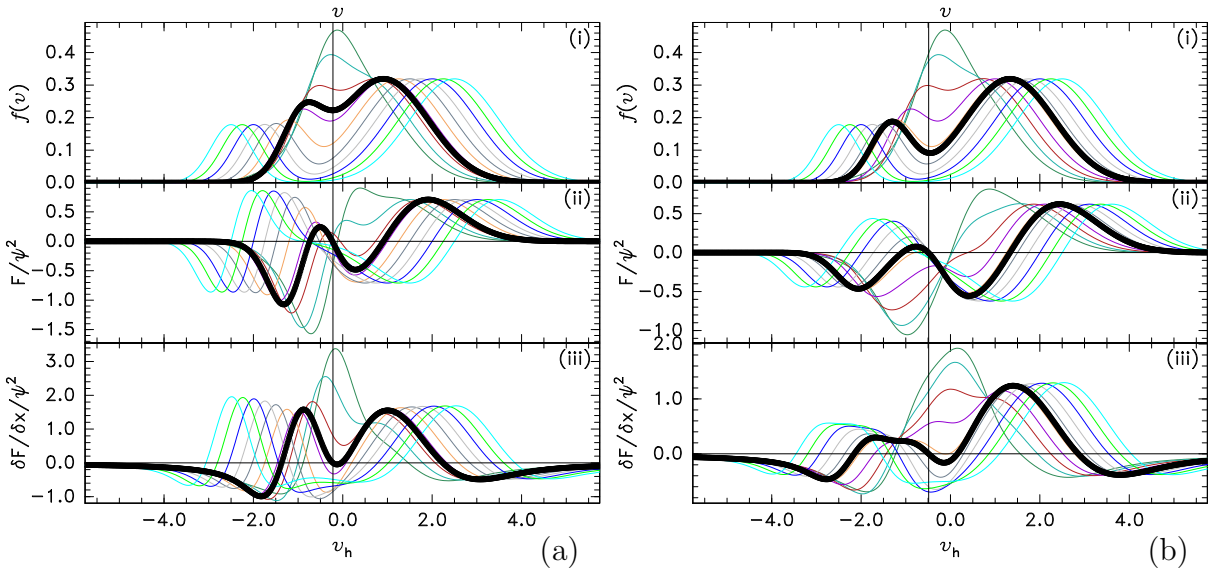

Figure 4: Distribution function (i) $f(v)$, force (ii) $F(v_h)$, and stability coefficient (iii) $\delta F/\delta x$, as a function of velocity (v and v_h), for a range (different colors) of distribution beam shift parameter v_b. Thick black line is the threshold case for stable electron hole existence. (a) $\psi = 0.02$, (b) $\psi = 0.5$.

equilibrium and the first that did permit it as the lower and upper limits of a new scan of v_b with the same number of steps (hence much smaller steps). Refined scans are not plotted. This process of decreasing the step size by a factor equal to the number of steps in the scan is iterated; when 10 steps are taken, two more iterations are enough to converge within other uncertainties. The stable case of the final v_b scan is interpolated for the threshold, and is plotted in thick black. The vertical line indicates the stable structure velocity v_{h0}.

It is observed in this and all other cases explored that the stable v_{h0} lies within a distribution function local depression but not necessarily exactly at the velocity of minimum $f(v)$. A stable electron hole equilibrium is found only if there exist three stationary points (two maxima and one minimum between them) of $f(v)$, and v_{h0} always lies between the locations of the maxima. It is also found that the required fractional depth of the minimum increases as ψ is increased, as the comparison between (a) and (b) of Fig. 4 illustrates.

A wider-ranging graphical impression of the range of marginal distribution shapes is given by Fig. 5. Each frame shows marginally stable distributions for $\psi = 0.05$ (green)

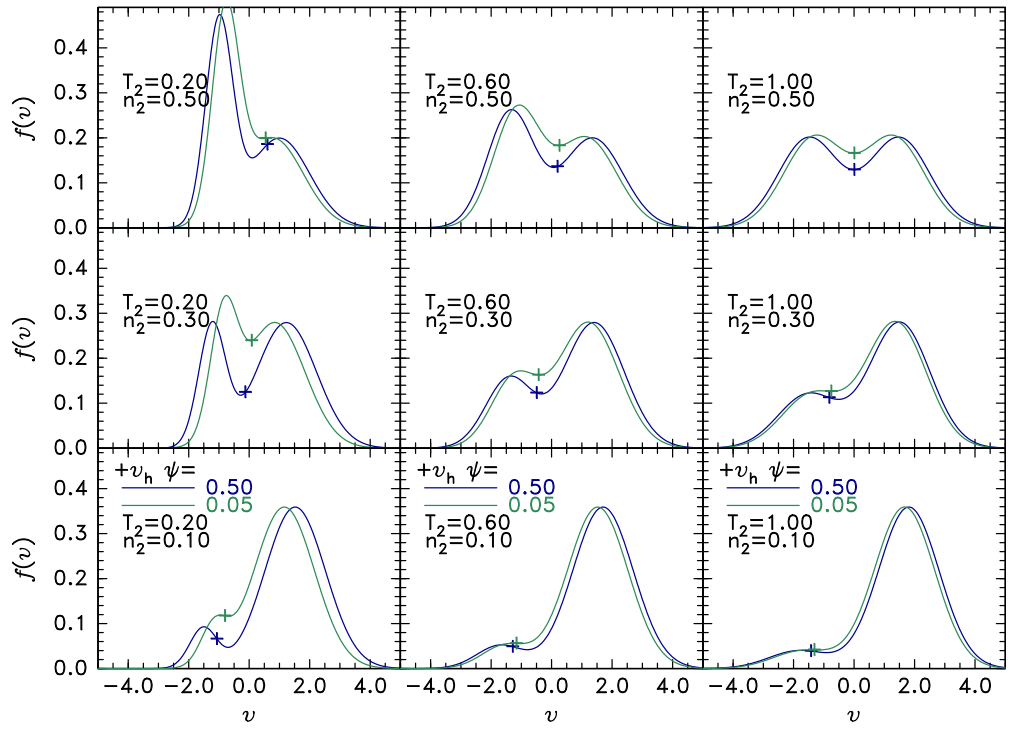

Figure 5: A range of marginal ion distribution shapes for two-Maxwellian distributions.

and $\psi = 0.5$ (blue), for different temperature T_2 and fractional density n_2 of the second Maxwellian component (toward negative v). The first component has $T_1 = 1$ and $n_1 = 1-n_2$. The equilibrium hole velocity v_{h0} is shown by the cross.

An estimate of the size of the damping coefficient b can be obtained by the observation that the typical value of dF/dv_h in plots like Fig. 4 is of order $-0.5\psi^2$ or smaller. Since the dimensionless hole mass is $M = -(m_eT_0/m_iT_e)\int \phi dx = -(m_eT_0/m_iT_e)L\psi$ and typically $L = (16/3)\sqrt{T_e/T_0}$ we have

$$|b| = \left|\frac{dF}{Mdv_h}\right| \lesssim 0.1\frac{m_i}{m_e}\sqrt{\frac{T_e}{T_0}}\psi. \tag{15}$$

This is rather comparable to the maximum absolute value of c in ion dimensionless units,

$$|c| = \left|\frac{\delta F}{M\delta x}\right| \lesssim \left(\frac{3}{16}\right)^2\frac{m_i}{m_e}\psi, \tag{16}$$

for $\sqrt{T_e/T_0}$ not much different from unity. The large values of both would mean that harmonic solutions would in fact be more than critically damped. However, since the resulting timescales are very short compared with $1/\omega_{pi}$, the mechanism of the ion density perturbation perfectly changing with hole motion as if in steady-state, giving rise to (b), is liable to be a very poor quantitative approximation, unlike the stationary ion mechanism (c) which is the opposite extreme. Nevertheless, the fact of b's sign being that of damping is an important indication that slow hole motions with c near zero will in fact be stable. A proper treatment for arbitrary frequency, of course, requires solution of the time-dependent Vlasov equation for ions, which is not attempted here.

4 Ion Distribution Linear Stability

The background one-dimensional warm two-beam ion distributions might experience sinusoidal linear electrostatic instability not caused by solitary structures, depending on the spacing, relative density, and velocity-width of the beams, and on the electron temperature[26, 27]. Generally this ion-ion instability requires a local minimum in the ion distribution of a certain depth. It is conceivable that such an instability might contribute to the mechanism that *forms* an electron hole, but that is not the focus here. However, the question arises as to whether the non-single-humped background plasma ion distribution *required for persistence* of slow electron holes is stable to ion-ion modes. If not, perhaps electron hole existence would be prevented because the required background distribution minimum is unstable. The ion-ion instability can be explained in outline, with reference to Fig 6 (obtained by a numerical method of analyzing and visualizing these and other kinetic ion instabilities for arbitrary ion distributions developed by the present author, mostly for pedagogic purposes [see `https://github.com/ihutch/chiofv`]). The one-dimensional ion velocity distribution being analysed is shown in the upper panel. The small middle panel shows the peak of the electron distribution function with temperature $T_e = T_0$, to indicate its very different velocity scale and the limited extent to which its gradient is significant.

For a wave of complex frequency ω, real wave number k, and thus phase velocity $v_p = \omega/k$ the lower panel shows contours on the complex phase velocity plane (scaled to an ion speed $\sqrt{T_0/m_i}$ where T_0 is a reference temperature) of the complex quantity $(k\lambda_D)^2\chi_i$; the Debye length is $\lambda_D = \sqrt{\epsilon_0 T_0/e^2 n_e}$, and χ_i is the ion susceptibility. For species j, the quantity

$$k^2\lambda_D^2\chi_j = -(\lambda_D\omega_{pj})^2 \int \frac{\partial f_j}{\partial v}\frac{1}{v - v_p}dv \ , \tag{17}$$

(integrating along the Landau contour) is a function only of the ion distribution shape and (complex) v_p, not of ω and k separately. The dispersion relation for electrostatic waves is $\chi = \chi_e + \chi_i = -1$. Therefore any solution must have the imaginary part of χ equal to zero. Contours of zero imaginary part of χ_i and of χ are shown in black and blue respectively. The electron susceptibility (for Maxwellian electron temperature T_e) gives to an excellent approximation $(k\lambda_D)^2\chi_e = (T_0/T_e)(1 + iv_p\sqrt{\pi m_e/2T_e})$, and contributes an adjustment to the imaginary part of χ at large $|\Re(v_p)|$, which is electron Landau damping of ion acoustic waves. But for the low velocity instability this contribution is negligible and the black and blue contours coincide.

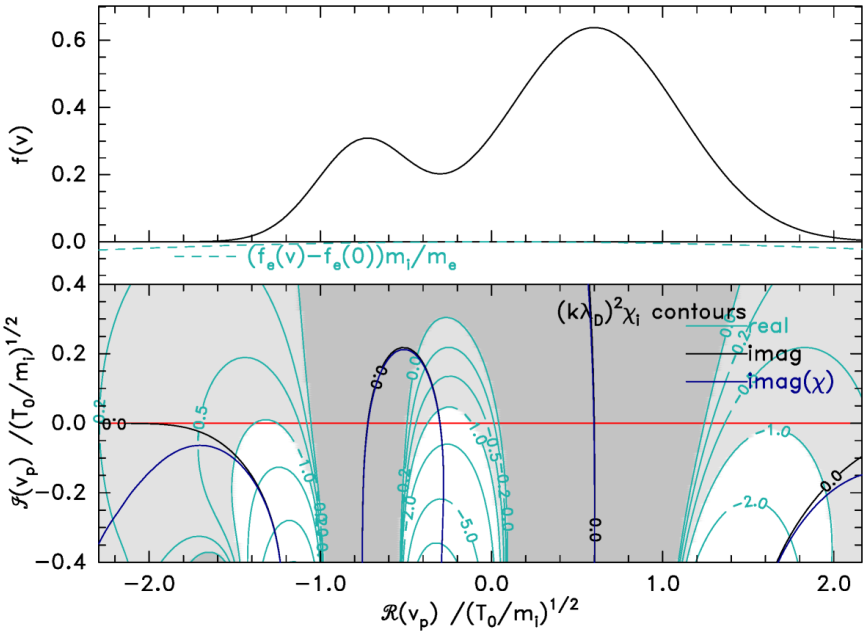

Figure 6: Contours of scaled susceptibility on the complex phase velocity plane. Dispersion relation solutions lie at intersections of the black or blue contours with the green contours. No solutions exist in dark shaded regions. Solutions exist in light shaded regions only for $T_e \geq T_0$.

The electron contribution to the real part of $(k\lambda_D)^2\chi$ is to an excellent approximation simply (T_0/T_e). And the real part of the dispersion relation is then $k^2\lambda_D^2 = -\Re(k^2\lambda_D^2\chi_i) - T_0/T_e$; so the intersection of the zero imaginary contour with a green contour indicates the value of dispersion solution's wavenumber. If k is regarded as a free choice, the dispersion relation can be satisfied for some k if $\Re(k^2\lambda_D^2\chi_i) + T_0/T_e$ is negative. Therefore the limiting solution of the dispersion relation as $k \to 0$ lies at $\Re(k^2\lambda_D^2\chi_i) = -T_0/T_e$, and when $T_e/T_0 \to \infty$ it is at $\Re(k^2\lambda_D^2\chi_i) = 0$. Where the appropriate contour of $\Re(k^2\lambda_D^2\chi_i)$ crosses the zero contour of $\Im(\chi)$ is the dispersion solution for v_p. If the intersection lies below the real axis, the mode is damped; if above, it is growing (unstable). In regions where $\Re(k^2\lambda_D^2\chi_i)$ is positive, no solutions exist (regardless of non-negative electron temperature) and the plane is shaded dark gray. In regions where $\Re(k^2\lambda_D^2\chi_i) > -1$ no solution exists for $T_e \leq T_0$, and the regions where it lies between -1 and 0 are shaded light gray. The green contours for different negative values $-(0,.2,.5,1,2,5,10)$ of $\Re(k^2\lambda_D^2\chi_i)$ therefore correspond to boundaries of solution regions for $T_e = -T_0/\Re(k^2\lambda_D^2\chi_i)$.

Two-beam distributions like Fig. 6 have three unshaded regions where solutions exist. Those on the right and left are the positively and negatively propagating ion acoustic waves, lying below the real axis when electron Landau damping is included. The central region coinciding with the distribution local minimum is where ion-ion instability solutions lie. The stability of this ion-ion mode is not significantly influenced by electron Landau damping. Changing the electron temperature changes the stability not by changing the local electron distribution *gradient* but by changing its *height* (inversely with its overall width).

There is therefore a threshold electron temperature above which a (sufficiently) double-

humped ion distribution function becomes unstable. This temperature is a convenient way to parameterize the ion-ion stability of the distribution, and it can be found simply by examining $k^2\lambda_D^2\chi_i$ along the real v_p axis, and finding its real value at the velocity where its imaginary part is zero, giving $T_{threshold} = -T_0/\Re(k^2\lambda_D^2\chi_i)$. This is equivalent to the standard Nyquist stability analysis used in this context by Penrose[28], but expressed in a different way.

Fig. 7 shows contours of $T_{threshold}$ as a function of the distribution parameters. Those parameters are ordered like Fig. 5, which therefore shows qualitatively how the distribution shape changes over the contour plane. Higher $T_{threshold}$ are more stable cases. The first

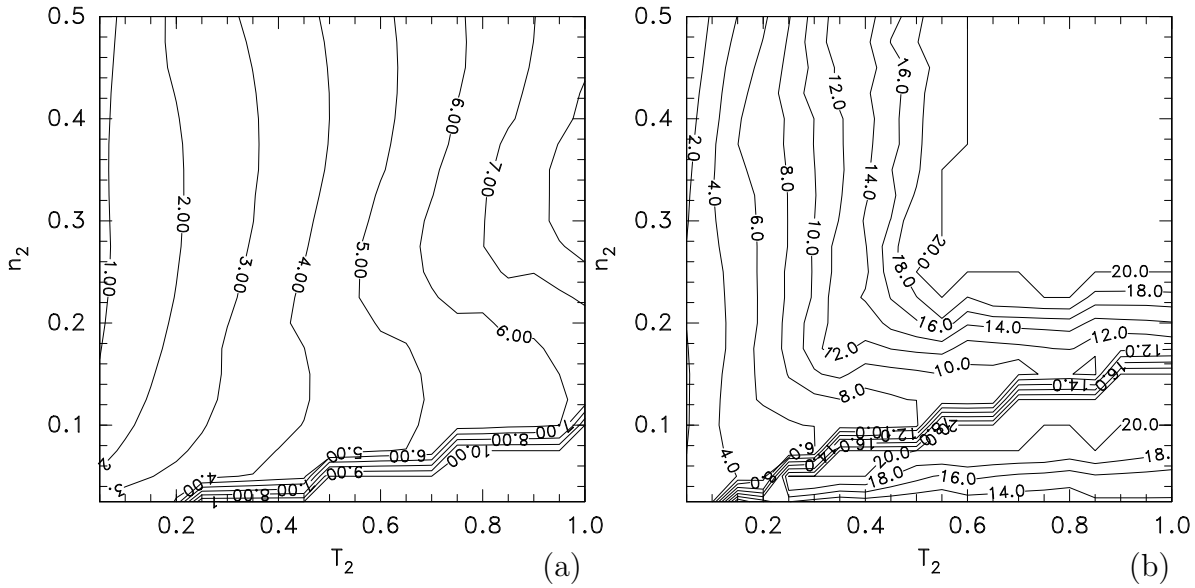

Figure 7: Contours of the electron temperature $T_{threshold}$ above which ion-ion instability occurs in two-Maxwellian distributions for which the first component has unit temperature and the second component temperature T_2 and fractional density n_2, and the shift between them is minimal for the existence of electron holes having (a) $\psi = 0.5$, and (b) $\psi = 0.1$.

component of the two-Maxwellian distribution has temperature $T_0 = 1$, and density $1 - n_2$, where n_2 is the total density of the second component, whose temperature is T_2. Thus n_2 and T_2 together determine the shape of the distribution, because the component velocity separation $2|v_b|$ is found by the process described in section 3.2. In other words $|v_b|$ is taken to be the minimum that allows the persistence of an electron hole. Fig. 7(a) is for a large amplitude hole $\psi = 0.5$ which requires substantially deeper minimum in the distribution (larger $|v_b|$ and hence less stable) than Fig. 7(b). The value $\psi = 0.1$ (b) is representative of small ψ. The uncertainty level of perhaps a few percent in the threshold away from the sharp cliff probably arises from the discrete velocity meshes and from the relatively coarse parameter mesh 20×20. Since large $T_{threshold}$ occurs for some regions, contours are not shown above $T_{threshold} = 10$ (a) or 20 (b). Overall at the rather extreme large amplitude $\psi = 0.5$ (a), even for unusually small T_2 no instability occurs for $T_e \gtrsim T_0$ or in fact for $T_e \gtrsim 6T_{min}$, where T_{min} is the smaller of the two components' ion temperatures, no matter what n_2 is. For small amplitude holes ($\psi = 0.1$) (b), $T_{threshold} \gtrsim 20T_{min}$ over the great majority of the

plane, showing that the marginal distribution for the existence of small amplitude holes is highly stable to the ion-ion mode.

5 Conclusions

Long-lived one-dimensionally stable slow electron hole equilibria can exist only when the background ion velocity distribution has a sufficiently deep local minimum and the electron hole speed lies within it. If the electron temperature is less than ~ 6 to 20 times the effective temperature of the colder ion component, then the required background ion distribution will be linearly stable; so there is no (linear electrostatic, 1-D) stability reason it should not exist. The ion density change caused by a solitary positive potential peak whose velocity lies in the local minimum, is positive, avoiding the self-acceleration of the hole that otherwise occurs. However, ion charge perturbations alone cannot create the conditions for a *slow* positive soliton, and the electron charge perturbation of a distribution without phase-space-density deficit in the trapped region cannot permit a total charge density positive at the potential peak and negative in the wings, as is required for a soliton. Therefore is seems that persistent, slow, positive, solitary potential structures must be sustained primarily by trapped electron deficit. That is, they must be electron holes. And their velocity must lie in a local minimum in the ion velocity distribution. It is not impossible that slow electron holes might be observed as they form, or shortly afterwards, in ion distributions that do not possess the local minimum found here. But they would be expected to be unstable, and so rapidly be self-accelerated to speeds that are no longer slow.

All of the analysis presented here is purely one-dimensional. However, it seems possible that the ion coupling effects explored also have a significant effect on the multidimensional transverse stability of electron holes, quite possibly helping to stabilize it. If so, then slow electron holes might prove to have different typical transverse sizes than fast electron holes, or even to persist at lower magnetic field strengths.

Acknowledgements

I am grateful to I Y Vasko, Y Kamaletdinov, and A V Artemyev for stimulating discussions of slow electron holes, especially their recent analysis of MMS observations confirming that they lie in minima of $f_i(v)$. The present work was not supported by any external public funding. The code used to calculate and plot the figures may be found at `https://github.com/ihutch/slowholes`; no data was used.

References

[1] D B Graham, Yu V Khotyaintsev, A Vaivads, and M André. Electrostatic solitary waves and electrostatic waves at the magnetopause. *Journal of Geophysical Research: Space Physics*, 121:3069–3092, 2016.

[2] K. Steinvall, Yu. V. Khotyaintsev, D. B. Graham, A. Vaivads, P.-A. Lindqvist, C. T.

Russell, and J. L. Burch. Multispacecraft analysis of electron holes. *Geophysical Research Letters*, 46(1):55–63, 2019. URL https://agupubs.onlinelibrary.wiley.com/doi/abs/10.1029/2018GL080757.

[3] A. Lotekar, I. Y. Vasko, F. S. Mozer, I. Hutchinson, A. V. Artemyev, S. D. Bale, J. W. Bonnell, R. Ergun, B. Giles, Yu. V. Khotyaintsev, P.-A. Lindqvist, C. T. Russell, and R. Strangeway. Multisatellite mms analysis of electron holes in the earth's magnetotail: Origin, properties, velocity gap, and transverse instability. *Journal of Geophysical Research: Space Physics*, 125(9): e2020JA028066, 2020. URL https://agupubs.onlinelibrary.wiley.com/doi/abs/10.1029/2020JA028066. e2020JA028066 10.1029/2020JA028066.

[4] Hans Schamel. Electrostatic Phase Space Structures in Theory and Experiment. *Physics Reports*, 140(3):161–191, 1986.

[5] I H Hutchinson. Electron holes in phase space: What they are and why they matter. *Physics of Plasmas*, 24(5):055601, may 2017. URL http://aip.scitation.org/doi/10.1063/1.4976854.

[6] I H Hutchinson and C Zhou. Plasma electron hole kinematics. I. Momentum conservation. *Physics of Plasmas*, 23(8):82101, 2016. URL http://dx.doi.org/10.1063/1.4959870.

[7] C Zhou and I H Hutchinson. Plasma electron hole kinematics. II. Hole tracking Particle-In-Cell simulation. *Physics of Plasmas*, 23(8):82102, 2016. URL http://dx.doi.org/10.1063/1.4959871.

[8] Chuteng Zhou and Ian H Hutchinson. Plasma electron hole ion-acoustic instability. *J. Plasma Phys.*, 83:90580501, 2017.

[9] Koichi Saeki and J Juul Rasmussen. Stationary solution of coupled electron hole and ion soliton in a collisionless plasma. *Journal of the Physical Society of Japan*, 60(3): 735–738, 1991.

[10] Koichi Saeki and Hitoshi Genma. Electron-Hole Disruption due to Ion Motion and Formation of Coupled Electron Hole and Ion-Acoustic Soliton in a Plasma. *Physical Review Letters*, 80(6):1224–1227, feb 1998.

[11] Chuteng Zhou and Ian H. Hutchinson. Dynamics of a slow electron hole coupled to an ion-acoustic soliton. *Physics of Plasmas*, 25(8):082303, 2018. URL http://aip.scitation.org/doi/10.1063/1.5033859.

[12] C Norgren, M André, D B Graham, Yu V Khotyaintsev, and A Vaivads. Slow electron holes in multicomponent plasmas. *Geophysical Research Letters*, 42(18):7264–7272, 2015.

[13] C Norgren, M André, A Vaivads, and Y V Khotyaintsev. Slow electron phase space holes: Magnetotail observations. *Geophysical Research Letters*, 42(6):1654–1661, 2015.

[14] J F Drake, M Swisdak, C Cattell, M A Shay, B N Rogers, and A Zeiler. Formation of electron holes and particle energization during magnetic reconnection. *Science (New York, N.Y.)*, 299(5608):873–877, 2003. URL http://www.ncbi.nlm.nih.gov/pubmed/12574625.

[15] Yu V Khotyaintsev, A Vaivads, M André, M Fujimoto, A Retinò, and C J Owen. Observations of slow electron holes at a magnetic reconnection site. *Physical Review Letters*, 105(16):165002, 2010.

[16] L Muschietti, I Roth, R E Ergun, and C W Carlson. Analysis and simulation of BGK electron holes. *Nonlinear Processes in Geophysics*, 6(3/4):211–219, 1999. URL http://www.nonlin-processes-geophys.net/6/211/1999/npg-6-211-1999.html.

[17] B Eliasson and P K Shukla. Dynamics of electron holes in an electron-oxygen-ion plasma. *Physical Review Letters*, 93(4):45001, jul 2004. URL http://journals.aps.org/prl/abstract/10.1103/PhysRevLett.93.045001.

[18] B Eliasson and P K Shukla. Formation and dynamics of coherent structures involving phase-space vortices in plasmas. *Physics Reports*, 422(6):225–290, jan 2006. URL http://linkinghub.elsevier.com/retrieve/pii/S037015730500390X.

[19] Christian Bernt Haakonsen, Ian H Hutchinson, and Chuteng Zhou. Kinetic electron and ion instability of the lunar wake simulated at physical mass ratio. *Physics of Plasmas*, 22 (3):32311, mar 2015. URL http://scitation.aip.org/content/aip/journal/pop/22/3/10.1063/1.4915525.

[20] Amar Kakad, Bharati Kakad, Chandrasekhar Anekallu, Gurbax Lakhina, Yoshiharu Omura, and Andrew Fazakerley. Slow electrostatic solitary waves in earth's plasma sheet boundary layer. *Journal of Geophysical Research: Space Physics*, 121(5):4452–4465, 2016. URL https://agupubs.onlinelibrary.wiley.com/doi/abs/10.1002/2016JA022365.

[21] Thomas H Dupree. Theory of phase-space density holes. *Physics of Fluids*, 25(2): 277, 1982. URL http://scitation.aip.org/content/aip/journal/pof1/25/2/10.1063/1.863734.

[22] Debraj Mandal, Devendra Sharma, and Hans Schamel. Ultra slow electron holes in collisionless plasmas: Stability at high ion temperature. *Physics of Plasmas*, 27(2): 022102, 2020. URL https://doi.org/10.1063/1.5121530.

[23] T H Dupree. Growth of phase-space density holes. *Physics of Fluids*, 26(9): 2460, 1983. URL http://scitation.aip.org/content/aip/journal/pof1/26/9/10.1063/1.864430.

[24] I B Bernstein, J M Greene, and M D Kruskal. Exact nonlinear plasma oscillations. *Physical Review*, 108(4):546–550, 1957. URL http://journals.aps.org/pr/abstract/10.1103/PhysRev.108.546.

[25] M A Raadu. The physics of double layers and their role in astrophysics. *Physics reports*, 178(2):25–97, 1989. URL http://www.sciencedirect.com/science/article/pii/0370157389901099.

[26] T E Stringer. Electrostatic instabilities in current-carrying and counterstreaming plasmas. *Journal of Nuclear Energy. Part C, Plasma Physics*, 6:267–279, 1964. URL http://iopscience.iop.org/0368-3281/6/3/305.

[27] B D Fried and A Y Wong. Stability Limits for Longitudinal Waves In Ion Beam-Plasma Interaction. *Physics of Fluids (1958-1988)*, 9:1084–1089, 1966. URL http://scitation.aip.org/content/aip/journal/pof1/9/6/10.1063/1.1761806.

[28] Oliver Penrose. Electrostatic Instabilities of a Uniform Non-Maxwellian Plasma. *Physics of Fluids*, 3(2):258, 1960. URL http://scitation.aip.org/content/aip/journal/pof1/3/2/10.1063/1.1706024.